

# CRAFT: Long-Horizon Cable Routing Algorithm and Low-Friction Caging Gripper

Ziyang Chen, *Member, IEEE*, Yash Chitambar, Theodore Lam,  
Hui Li, Sachin Chitta, Ken Goldberg, *Fellow, IEEE*

**Abstract**—Cable routing is a common manipulation task in assembly and manufacturing, yet it remains challenging due to the deformable nature of cables and the constraints of cluttered routing environments. In this paper, we present CRAFT: Cable Routing Around Fixtures using Two grippers, a novel hardware plus software architecture that integrates unimanual and bimanual operations for long-horizon cable routing. To address jamming due to friction, we present a novel caging gripper with roller mechanism. Physical experiments consisting of 160 trials on a modified NIST board with five types of fixtures and turning angle up to 930 degrees, yield an average completion ratio of 84.5% across four routing difficulty tiers, representing a 54.2% improvement over an earlier baseline. The cable routing materials and benchmarks are available at [https://manipulation-net.org/tasks/cable\\_routing.html](https://manipulation-net.org/tasks/cable_routing.html).

## I. INTRODUCTION

Cable routing, the task of manipulating Deformable Linear Objects (DLOs) such as wires, hoses, or cables, is important for a wide range of technological applications. For example, cable routing is performed during many assembly operations, when wiring servers in data centers, for cable harnesses in automobiles, and suturing in surgery [1]–[4]. Robotic cable manipulation in these contexts requires methodical planning of cable paths before routing and advanced control of DLOs during execution. Since DLOs exhibit complex behaviors like bending, twisting, and tangling when manipulated, the task of routing a cable into a desired configuration is complicated. These effects become more apparent in long-horizon cable routing, where, due to the length of the cable, small deviations from the desired cable placement can lead to significant routing errors [5]. Additionally, friction between the gripper and the cable hinders smooth sliding and effective slack management. As a result, automated cable routing remains an open and demanding problem.

We present CRAFT: Cable Routing Around Fixtures using Two grippers, a novel cable routing framework integrating unimanual and bimanual operations for routing cables through different types of fixtures on a planar surface. We design a low-friction caging gripper to enable smooth cable sliding. Given an overhead RGB image of fixtures and a desired routing path, CRAFT plans a sequence of grasping,

Ziyang Chen, Yash Chitambar, Theodore Lam, and Ken Goldberg are with the Department of Electrical Engineering and Computer Sciences, University of California at Berkeley, Berkeley, CA 94709, USA. [ziyang.chen@berkeley.edu](mailto:ziyang.chen@berkeley.edu)

Hui Li, and Sachin Chitta are with Autodesk Research, San Francisco, CA 94105, USA.

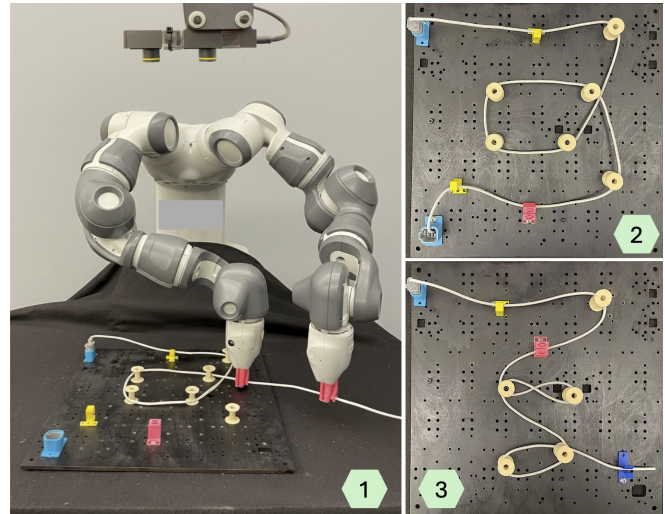


Fig. 1. CRAFT overview: (1) An ABB YuMi dual-arm robot with an overhead RGB camera, (2) and (3) show two Tier 4 cable routing configurations.

lifting, twisting, and sliding motions for two robot grippers and executes the resulting plan.

This paper makes 3 contributions:

- 1) A novel CRAFT gripper with integrated rollers designed to reduce friction between the cable and jaws during routing.
- 2) A novel CRAFT cable routing algorithm integrated with unimanual and bimanual operations for long-horizon cable routing.
- 3) Results from 160 physical experiments that suggest CRAFT can reliably route cables with up to 10 fixtures and 930 degrees of total turning angle, achieving an average completion ratio of 84.5%, which significantly outperforms an earlier baseline.

## II. RELATED WORK

### A. Robot deformable object manipulation

The manipulation of deformable objects, such as cables [6]–[8], cloth [9], [10], bags [11]–[13], and sutures [14], [15], is common in daily life, but remains difficult for robots. Challenges, such as identifying reliable interaction points, handling shape changes during manipulation, and ensuring stable grasping to avoid slipping, remain unsolved in this field [16], [17]. Some model-based approaches have been used. For example, Yan et al. [18] combined an optimized visual representation model and a dynamics model using contrast estimation to perform short-horizon deformable object

manipulation tasks such as spreading ropes and cloth. To implement a relatively long-horizon task, Chen et al. [15] developed a monocular visual servoing strategy to grasp sutures in surgery and performed double knot tying on an open chicken wound. However, they do not implement continuous perception to observe suture deformation during operation. Some recent works have focused on manipulating deformable objects using model-free approaches. Chen et al. [11] developed a self-supervised learning framework that enabled a bimanual robot to recognize the handle and rim of a plastic bag and open it through interactive manipulation to complete an object insertion task. Vision-Language-Action (VLA) models [19]–[21] have also been explored to enable robots to complete tasks via end-to-end robot control. This includes manipulation of deformable objects such as papers, towels and cloth, which shows promising results in terms of task and environment generalization. To compare the advantages between model-based and model-free strategies, Hoque et al. [9] benchmarked fabric manipulation by comparing four model-based algorithms and four model-free policies, and the results showed that combining learning with an analytical method could achieve nearly human-like performance in fabric flattening and folding, suggesting the potential of combining model-based and model-free solutions.

### B. Robotic adaptive grippers for object manipulation

Works on robotic gripper designs aim to address various aspects of object manipulation through sensing, grasp stability, or in-hand manipulation. Burgess et al. [22] and She et al. [8] explored integrating tactile sensing into parallel-jaw grippers, allowing for active force sensing solutions to cable manipulation. However, these approaches are bulky and mechanically complex, hindering routing maneuverability in dense routing environments and making bimanual cable manipulation difficult for tension regulation. Yuan et al. [23] and Bicchi et al. [24] presented active roller-based grippers that achieve high dexterity by allowing in-grasp rotation and effective management of contact forces. These systems are generally tuned for rigid object manipulation and haven't been tested to manipulate deformable objects. Goldberg and Furst [25] presented a gripper with passive linear bearing to avoid wedging in the sliding grasp plate. Similarly, Carlisle et al. [26] presented a gripper with passive rotational bearings aligned with the grasp axis that use gravity to pivot objects into desired orientations.

Viswanath et al. [27] developed grippers with “fingernails” optimized for picking up cables from flat surfaces, which perform well but struggle to control tension during routing, leading to slack accumulation and snagging. Lou et al. [28] introduced a flat clamping jaw solution that achieves consistent cable pickup but is limited to near-linear routing patterns. Recently, Zuo et al. [29] proposed a bio-inspired claw design that mimics an eagle nail to lift cables. Although this design is effective for some tasks, such as adjusting the position of the cable, it does not consider highly compliant cables, which may fold or stack due to the friction between the cable and the gripper during routing, particularly when

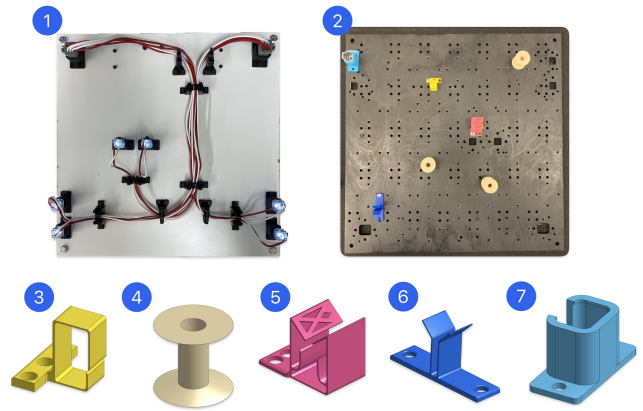


Fig. 2. NIST Board and the fixtures: 1) Standard NIST Task Board, 2) Modified NIST Board with fixtures, 3) C-clip, 4) Round Peg, 5) U-clip, 6) Y-clip, 7) Connector.

there are large orientation changes between fixtures.

### C. Robotic cable routing

Robotic cable routing introduces additional challenges in deformable object manipulation, for example, the cable needs to be routed around multiple fixtures in a cluttered environment while maintaining proper control of tension and slack [30]. Saha et al. [31] and Waltersson et al. [32] introduced bimanual cable routing operations, but did not address the issue of cable tension. Suberkrub et al. [33] proposed cable manipulation by using force information based on wrist force-torque sensors, and the experimental results showed that this approach can measure cable tension during routing and insertion into clamps. In experiments, the routing board configurations were relatively simple with total turning angle of up to 360 degrees.

Some recent works have also used data-driven strategies to train cable routing policies that generate action sequences of coordinated robot movements [6]. For example, Luo et al. [28] developed a hierarchical policy for cable routing that includes a high-level policy to select specific motion primitives such as pickup, route and perturb, and also a low-level policy to execute specific robot actions. Their approach demonstrated the feasibility of cable routing, but the routing configurations are limited to three fixtures with total turning angle of 180 degrees.

Most recently, Azulay et al. proposed MOTORCYCLE 1.0 [34], which implemented cable routing using bimanual sliding motions. They developed a collaborative working mode in which one leading arm was used to route the cable and another following arm was used to manage slack by lifting the cable. However, physical experiments involving five fixtures with turning angles up to 410 degrees showed that there was significant friction on the grippers in high-curvature regions, preventing long-horizon cable routing.

## III. PROBLEM STATEMENT

We make the following assumptions:

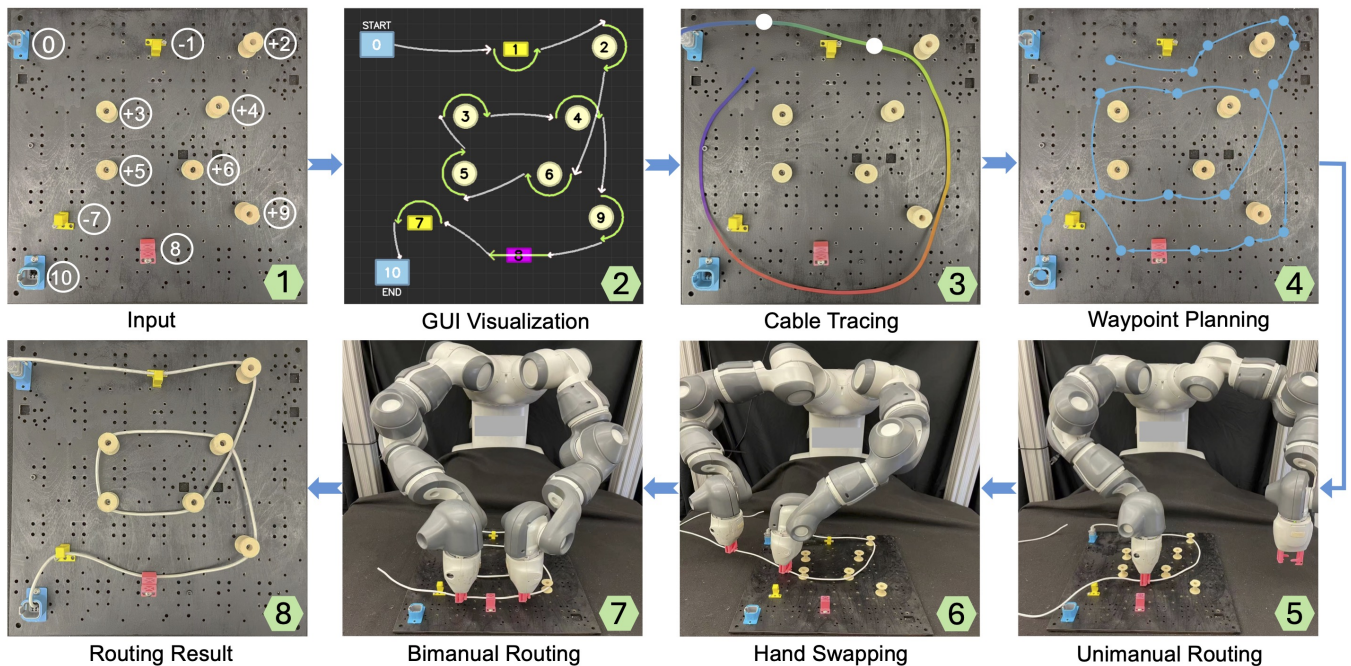


Fig. 3. Overview of the CRAFT pipeline: (1) input including an RGB board image with fixtures and a desired routing configuration  $C$ ; (2) An interface visualized for the user before physical cable routing; (3) Cable tracing to identify two initial grasp points on the cable; (4) A series of waypoints planned for cable routing; (5), (6) and (7) demonstrate the different primitives of cable routing, including unimanual routing, hand swapping, and bimanual routing; (8) The physical result of cable routing.

1) Given one cable, a planar worksurface, and up to 10 fixtures mounted on the worksurface.

2) The cable and worksurface are visually distinguishable and the cable is not tangled at the initial state.

3) One end of the cable is attached to a fixed connector, and the other end is unconstrained.

4) All fixtures are within the robot's reachable workspace.

5) The fixture routing configuration  $C$  is feasible, for example, there are no two consecutive fixtures with the same ID to be routed.

Following the NIST cable routing standard in Fig. 2.1, we assume a planar fixture board with an  $n \times n$  grid of mounting holes and  $N$  fixtures, such that there is clearance of  $Y$  between any two fixtures. The input includes:

1) An RGB image captured by the overhead camera. A Graphical User Interface (GUI) is provided for the operator to manually annotate the fixtures on the board to generate a fixture arrangement  $A$ , containing a set of fixtures, each of which includes three variables: a) an integer index from 0 to  $N$ ; b) the type of fixture (peg, C-clip, connector, U-clip and Y-clip); c) the grid position  $(x, y)$  on a plane grid surface, as well as the orientation for U-clip and Y-clip.  $F_0$  is assumed to be the starting attachment point for one end of the cable.

2) A desired fixture routing configuration  $C$  defined by a sequence of signed integers  $\langle 0, -1, +2, 8, -7, 10 \rangle$ , where the sign indicates the direction of cable wrapping (i.e. + for clockwise, - for counter-clockwise). The U-clip and Y-clip are routed via vertical insertion according to their orientation and are therefore not assigned a sign.

The output is a cable routing plan: a sequence of bimanual

robot motion commands that can produce the desired cable routing configuration  $C$ . During physical experiments, if the robot fails to route the cable around a specific fixture, or the gripper drops the cable, the robot is stopped manually.

#### IV. METHODOLOGY

We present CRAFT, a hardware and software framework for long-horizon cable routing. The software pipeline is shown in Fig. 3. Given the input including an RGB image and a desired routing configuration  $C$ , CRAFT generates an interface that allows users to observe the desired cable routing result. It then produces physical action sequences for the dual-arm robot to route the cable. The specific hardware and software designs are explained below.

##### A. Hardware design

1) The modified NIST board and the fixtures

To evaluate cable manipulation performance, we created a modified version of the NIST Assembly Task Board 4 [35], a standardized benchmark for robotic cable routing. We designed 5 fixture types: 1) Cylindrical Peg, 2) C-Clip, 3) U-Clip, 4) Y-Clip, 5) Connector, as shown in Fig. 2. The pegs and C-clips are common fixtures used to constrain the cable, the U-clip is a type of clamp that requires bimanual operation for insertion, and the Y-clip and connector are used as endpoints requiring bimanual and unimanual operation, respectively. The modified board has the same dimensions as the NIST board, while has been perforated with many holes for mounting the different types of fixtures, to accommodate greater complexity in the routing.

2) CRAFT gripper

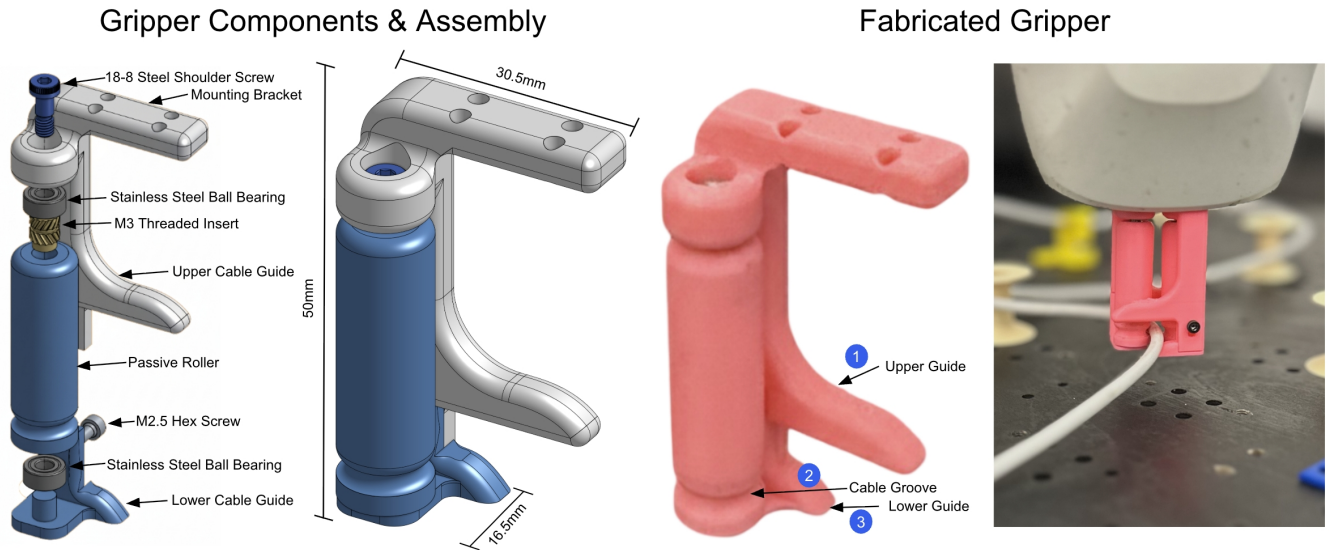


Fig. 4. CRAFT Gripper Assembly. *Left*: Exploded view and assembled view of mechanical components in the CRAFT Gripper. *Right*: Key features of CRAFT Grippers: 1) Upper Guide 2) Cable Groove 3) Lower Guide. Fabricated CRAFT Gripper jaws printed using polylactic acid (PLA) filament and installed on an ABB robot.

Reliable cable grasping is essential for consistent routing. CRAFT gripper has two identical jaws as shown in Fig. 4. Each jaw has two lower horizontal guides that can slide underneath a cable to help lift it from a worksurface. The upper horizontal guide ensures caging: preventing the cable from escaping when the jaws are closed. To manage cable tension, each jaw of the CRAFT gripper integrates a passive vertical roller mechanism. The roller is mounted on an axel with press-fitted bearings, allowing it to spin with minimal friction. The cable grooves ingrained into the roller increases surface contact with the cable to help the cable remain stably seated within the roller throughout a routing motion. Each CRAFT jaw consists of five COTS components and three 3D-printed components and can be assembled in under a few minutes.

### B. Software design

Let the board surface be defined as  $xy$ -plane with the  $z$ -axis pointing upward, and its  $z$  value is  $z_0$ . The 3D coordinates of the previous, current, and next fixtures are  $P_i$ ,  $P_{i+1}$  and  $P_{i+2}$ , respectively, with same  $Z$  values  $z_0$ . The distance between the previous fixture and the current fixture is denoted by  $d(P_i, P_{i+1})$ . The parameters used in the algorithm are explained in Table I. There is a variable length initial section where the cable is non-planar: at the attachment point  $F_0$ , the cable rises out of the planar worksurface due to the connector, which orients the cable upward before the cable drapes back down onto the plane, so two grippers are used to route the cable from  $F_0$  to  $F_1$ . The following gripper close to  $F_0$  is defined as  $G_F$ , and the leading gripper relatively far from  $F_0$  is defined as  $G_L$ .

#### 1) Initial cable tracing

To automatically determine initial grasp points on the cable for two grippers, we use HANDLOOM [36], a trained autoregressive cable tracing approach, to trace the initial state

TABLE I

CRAFT EMPIRICALLY-DETERMINED PARAMETERS THROUGH PRE-EXPERIMENTS.

Parameter	Definition
$h$	Height of the fixture
$r$	Outer radius of the round peg
$\omega$	Scaling factor to control cable lifting height
$\mu$	Scaling factor to overshoot the peg
$\lambda, \sigma, \alpha, \beta$	Scaling factor to control cable pulling length
$m$	Scaling factor to control the gripper rotation angle
$\gamma$	Distance offset between the gripper and the U-clip
$\phi$	Orientation of the U-clip on the $xy$ -plane
$\tau$	scaling factor to select a point close to the peg

of the cable. This model generates a probability map in each iteration and greedily selects the next cable pixel point based on the highest probability. CRAFT starts with  $F_0$ , and uses HANDLOOM to trace the cable and locate two grasp points on the cable: one at a distance equal to half the distance between  $F_0$  and  $F_1$  (grasping with the following gripper  $G_F$ ), and the other one at a distance equal to the distance between  $F_0$  and  $F_1$  plus half the distance between  $F_1$  and  $F_2$  (grasping with the leading gripper  $G_L$ ). The grippers are perpendicular to the cable path.

#### 2) Cable routing algorithm

After dual-arm grasping at the initial stage, the following gripper  $G_F$  moves to the midpoint between  $F_0$  and  $F_1$ , and the leading gripper  $G_L$  uses the unimanual cable routing plan to route the cable around  $F_1$ . Then,  $G_F$  releases the cable and  $G_L$  continues the routing process. Three different cable routing primitives, including unimanual, bimanual and hand-swapping plans, are explained below,

2.1) Fig. 5 illustrates the unimanual cable routing plan: the action sequences for routing the cable around each fixture (peg and C-clip) are formulated,

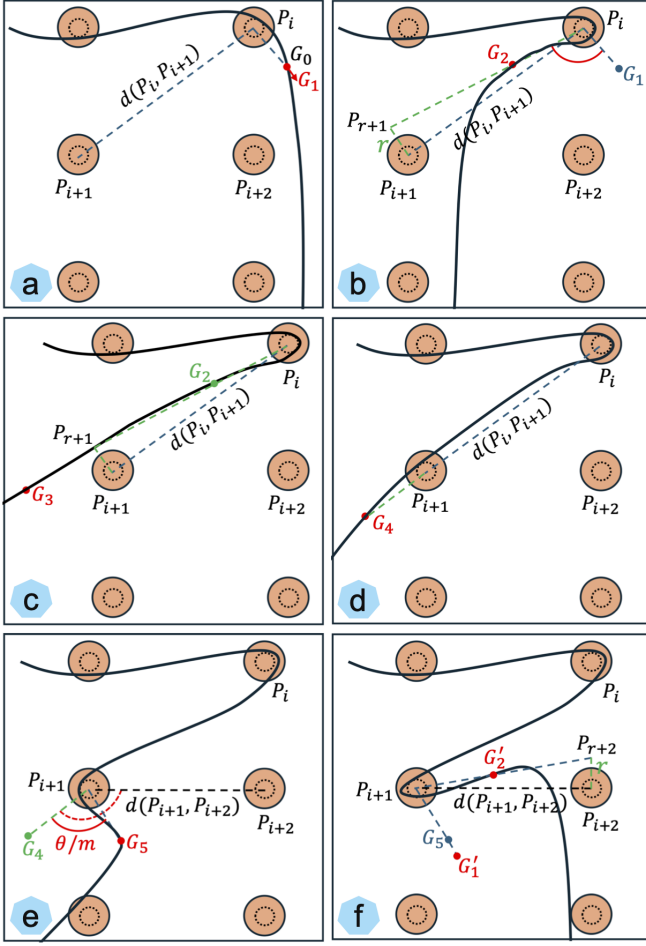


Fig. 5. 6 steps of the unimanual cable routing plan. The orange circle represents a round peg. The leading gripper  $G_L$  lifts the cable, rotates it to the next peg, pulls out the cable to reduce slack and routes it around the next peg.

(a) Starting from the initial position  $G_0(x, y, z)$  of the leading gripper,  $G_L$  slides to position  $G_1$  to reduce cable slack and lifts it above the fixtures:

$$G_1(x, y) = P_i(x, y) + \lambda d(P_i, P_{i+1}) \frac{G_0(x, y) - P_i(x, y)}{\|G_0(x, y) - P_i(x, y)\|},$$

$$G_1(z) = z_0 + \omega h, \quad \lambda \in (0, 1), \quad \omega > 1$$
(1)

(b) The leading gripper  $G_L$  routes the cable to position  $G_2$ :

$$P_{r+1} = P_{i+1} + \mu r \vec{n}_{r+1}, \quad \mu > 1$$

$$G_2(x, y) = P_i(x, y) + \sigma d(P_i(x, y), G_1(x, y)) \frac{P_{r+1} - P_i}{\|P_{r+1} - P_i\|},$$

$$G_2(z) = G_1(z), \quad \sigma > 1$$
(2)

Where  $\vec{n}_{r+1}$  is the normal vector perpendicular to the vector from  $P_i$  to  $P_{i+1}$ .

(c) The leading gripper  $G_L$  slides along the cable to

position  $G_3$  and overshoots the current peg:

$$G_3(x, y) = P_i(x, y) + \alpha d(P_i, P_{i+1}) \frac{P_{r+1} - P_i}{\|P_{r+1} - P_i\|}, \quad \alpha > 1$$

$$G_3(z) = G_2(z)$$
(3)

(d) The leading gripper  $G_L$  moves the cable to position  $G_4$  to make contact with the current peg:

$$G_4(x, y) = P_i(x, y) + \beta \|G_3(x, y) - P_i(x, y)\| \frac{P_{i+1} - P_i}{\|P_{i+1} - P_i\|},$$

$$G_4(z) = z_0, \quad \beta > 1$$
(4)

(e) The leading gripper  $G_L$  routes the cable around the current peg to position  $G_5$ :

$$\theta = \text{atan2}(u_x v_y - u_y v_x, u_x v_x + u_y v_y)$$

$$G_5(x, y) = P_{i+1}(x, y) + R(\theta/m) \cdot (G_4(x, y) - P_{i+1}(x, y))$$

$$G_5(z) = G_4(z), \quad m > 1$$
(5)

Where  $\vec{u} = P_{i+2} - P_{i+1}$  and  $\vec{v} = G_4 - P_{i+1}$ ,  $R$  is the rotation matrix.

(f) The leading gripper  $G_L$  repeats the action sequences, starting with a move to the new position  $G'_1$  and then routing the cable around the current peg until it reaches position  $G'_2$ . In this way,  $G_L$  can route the cable around a specific peg and move to the next one.

2.2) The bimanual cable routing plan for the U-clip (and the Y-clip) is illustrated in Fig. 6.

(a) The first step for the leading gripper  $G_L$  in transitioning to position  $G_1$  is the same as unimanual cable routing, to reduce cable slack and lift the cable above the current fixture.

(b) Based on the position  $P_{i+1}$  of the U-clip and its orientation  $\phi$  on the  $xy$ -plane, the goal position  $G_2$  of the leading gripper  $G_L$  is calculated as:

$$G_2(x, y) = P_{i+1}(x, y) + \text{sign}(\text{gripper}) \cdot \gamma \cdot (\cos(\phi), \sin(\phi))^T$$

$$G_2(z) = z_0 + \omega h$$
(6)

Where  $\text{sign}$  is a sign function, and it is 1 if the leading gripper  $G_L$  is the right gripper and  $-1$  with the left gripper.

(c) To generate a proper grasp point on the cable for the following gripper  $G_F$ , a point  $\tilde{P}_l$  on the connected line between the previous fixture and the leading gripper is calculated as:

$$\tilde{P}_l = P_i + \tau (G_2 - P_i), \quad 0 < \tau < 1$$
(7)

Then, the camera image is converted to grayscale and thresholded to extract the cable from the background. Starting from the projected pixel of  $\tilde{P}_l$ , a Breadth-First Search [37] algorithm is used to find the closest pixel on the cable. This pixel on the cable is used as the grasp point for the following gripper  $G_F$  and is projected to 3D space, denoted as  $\tilde{G}_3$ . Furthermore, a small window ( $15 \times 15$ ) is created, centered on the pixel point of  $\tilde{G}_3$ . A Random Sample Consensus (RANSAC) algorithm [38] is used to fit a line to the cable pixels within this window. The grasping orientation is perpendicular to the fitted line, which allows  $G_F$  to properly grasp the cable.

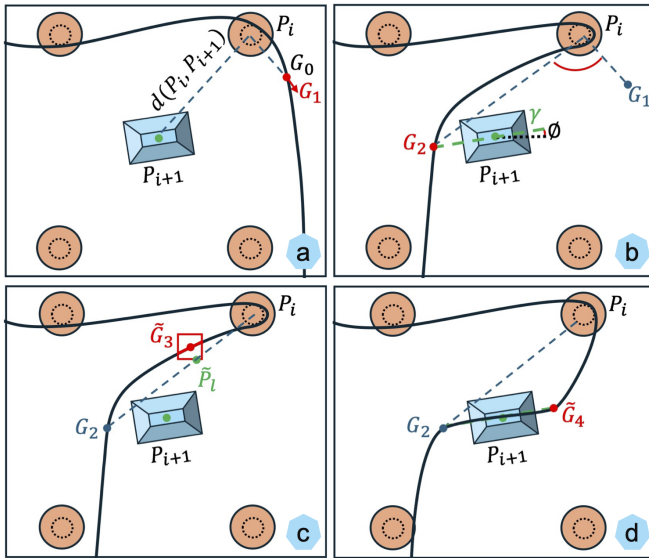


Fig. 6. 4 steps of the bimanual cable routing plan. The blue rectangle represents a U-clip that requires bimanual operation. The leading gripper  $G_L$  pulls the cable to one side of the U-clip, and the following gripper  $G_F$  grasps the cable and pulls it to the other side of the U-clip.

(d) The following gripper  $G_F$  moves to position  $\tilde{G}_4$  to align the cable with the centerline of the U-clip, and it is calculated using Formula (6) with an opposite sign value. Finally, the two grippers move downward a distance of  $wh$  to touch the board and insert the cable into the U-clip.

2.3) We use a hand swapping motion primitive to switch the cable-grasping gripper during routing. To implement this primitive, the leading gripper  $G_L$  pulls the cable out by a fixed distance to move away from the fixtures, and then the following gripper  $G_F$  grasps the cable using the same approach described in step (c) of the bimanual cable routing plan (2.2). There are two cases that can trigger the hand-swapping primitive:

- After routing the cable around  $F_1$  using two grippers to prevent the arched cable from slipping, the following gripper  $G_F$  releases the cable while the leading gripper  $G_L$  continues the routing process until the routing path changes direction (ie., the turning angle is greater than 90 degrees), hand swapping is triggered to swap the cable-grasping gripper.

- Some desired routing configurations have a 360-degree routing loop, which causes joint limit error with unimanual routing. To solve this, hand swapping is triggered after  $G_L$  has completed half of the loop, with  $G_F$  completing remaining half.

## V. PHYSICAL EXPERIMENTS

The experiments are conducted using an ABB YuMi IRB 14000 robot equipped with two CRAFT grippers. An overhead ZED mimi camera is mounted above the robot workspace (only RGB image is used as input), and a modified NIST board is placed on a table within the workspace for cable routing, as demonstrated in Fig. 1.

### 1) Fixture Routing Difficulty Metric

TABLE II

PERFORMANCE COMPARISON BETWEEN CRAFT AND BASELINE MOTORCYCLE 1.0 FOR 160 TRIALS (20 FOR EACH CONDITION). THE COMPLETION RATIO IS THE FRACTION OF FIXTURES CORRECTLY ROUTED. 'N/A' MEANS THAT THE APPROACH CANNOT ACHIEVE ANY CABLE ROUTING. CRAFT FULLY ROUTES ALL FIXTURES IN 55/80 TRIALS.

Metric	Method	Tier 1	Tier 2	Tier 3	Tier 4
Completion Ratio	MOTORCYCLE 1.0	53.2%	26.3%	23.6%	18.1%
	CRAFT	96.7%	87.8%	81.5%	71.9%
Execution Time (s)	MOTORCYCLE 1.0	108	N/A	N/A	N/A
	CRAFT	48	74	153	164

To quantitatively evaluate the difficulty of the cable routing task on the modified NIST board, we formulated a difficulty metric that considers the number of fixtures and the routing angles.

$$S = w_1 \frac{N_u + \eta N_b}{N} + w_2 \frac{\sum_{i=1}^{n-1} \theta_r}{\theta_{\max}} \quad (8)$$

Where  $N_u$  is the number of fixtures that rely on unimanual cable routing, including pegs, C-clips and connectors, while  $N_b$  is the number of fixtures with bimanual operation, including U-clips and Y-clips.  $N$  is the maximum number of fixtures in all routing configurations,  $\theta_r$  is the routing angle between two consecutive fixtures, and  $\theta_{\max}$  is the maximum routing angle by summing all routing angles.  $w_1$ ,  $w_2$ , and  $\eta$  are scaling factors to balance the task difficulty of unimanual and bimanual operation. In our experiments, the parameters were empirically set to the following values:  $w_1$  and  $w_2$  to 0.5,  $\eta$  to 2,  $N$  to 10, and  $\theta_{\max}$  to 1000 degrees.

Cable routing configurations are divided into four tiers based on the difficulty level: scores between 0 and 0.25 are categorized as Tier 1; scores between 0.25 and 0.5 are categorized as Tier 2; scores between 0.5 and 0.75 are categorized as Tier 3, and the most challenging case Tier 4 is with a score 0.75-1. Configurations with corresponding scores are illustrated in Fig. 7.

### 2) Experimental Protocol

To evaluate cable routing performance, we randomly sample four different routing configurations for each tier, and each configuration was executed five times. We used the recent work MOTORCYCLE 1.0 as the baseline and reproduced the caging gripper designed by the authors [34]. Both MOTORCYCLE 1.0 and CRAFT were evaluated using the same protocol, resulting in 160 physical experiments overall. In each experiment, we calculated the completion ratio (fraction of fixtures correctly routed) and the execution time.

Additionally, we extended the physical experiments to evaluate the effect of the caging gripper and the formulated cable routing algorithm. We sampled six routing configurations in different tiers where the previous baseline MOTORCYCLE 1.0 failed due to the torque limit, and executed cable routing five times for each configuration. For these

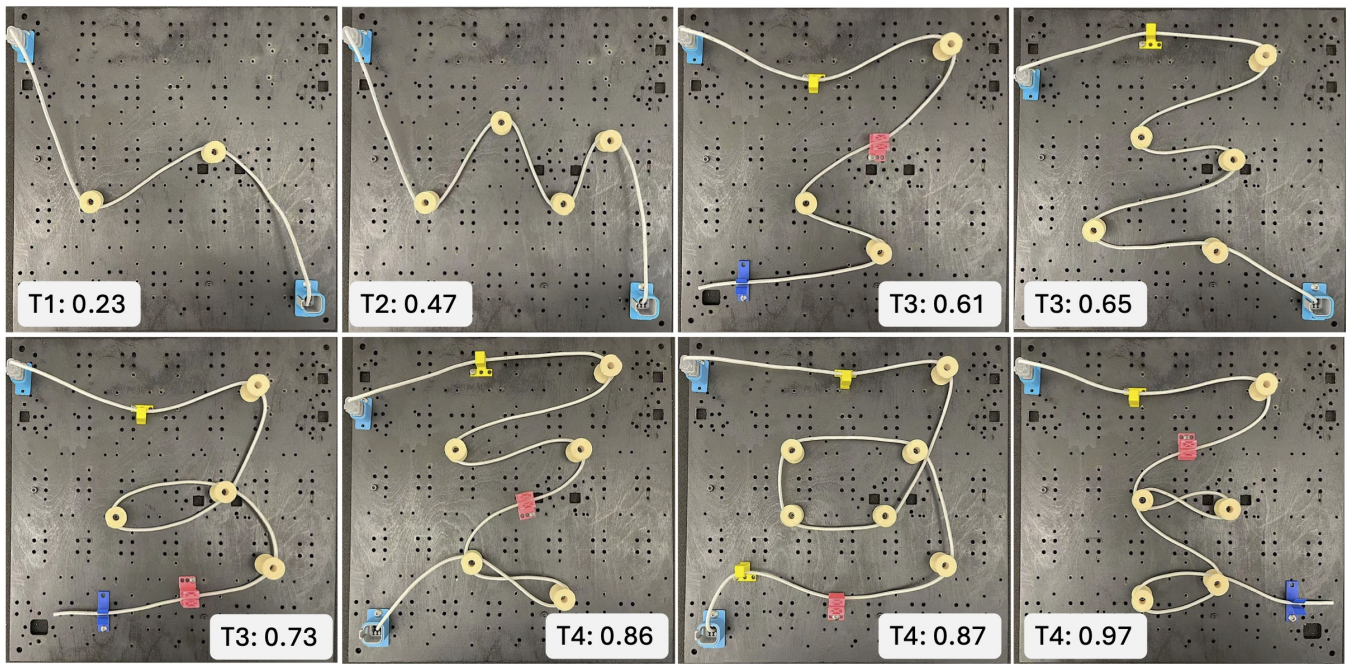


Fig. 7. 8 routing configurations with Tier difficulty level (1-4) and difficulty score (0.00-1.00).

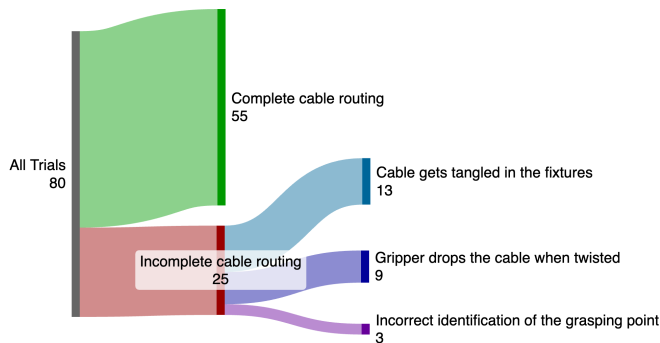


Fig. 8. A Sankey diagram of CRAFT failure modes for 80 trials.

extensive experiments, we used the designed low-friction caging gripper with the MOTORCYCLE 1.0 algorithm, and then the MOTORCYCLE 1.0 gripper with the CRAFT algorithm for cable routing.

### 3) Results

Table II shows a comparison study of cable routing based on routing configurations in different tiers. As shown in Fig. 8, the failure cases in CRAFT are due to three issues: 1) the cable tail gets tangled in the fixtures, preventing the gripper from moving to the next step, 2) the low-friction caging gripper drops the cable during routing, which is more evident when the cable is twisted at a large turning angle, and 3) the grasp point is not identified correctly during the bimanual operation. Regarding execution time, Table II shows that CRAFT can route the cable faster than MOTORCYCLE 1.0, approximately 10-20 seconds per fixture, mostly due to robot execution time. Table III shows an ablation study.

TABLE III  
ABLATION STUDY USING DIFFERENT COMBINATIONS OF CABLE ROUTING ALGORITHMS AND GRIPPERS IN 120 TRIALS (30 FOR EACH CONDITION).

Method	Completion Ratio
MOTORCYCLE 1.0	25.0%
MOTORCYCLE 1.0 Algorithm + CRAFT Gripper	33.9%
CRAFT Algorithm + MOTORCYCLE 1.0 Gripper	66.7%
CRAFT	88.3%

## VI. LIMITATIONS AND FUTURE WORK

In physical experiments, the CRAFT gripper sometimes dropped the cable. In future work, we will refine the gripper structure, such as integrating the eagle-fingernail gripper from [29]. Additionally, including a force sensor to perceive the grasping force may help dynamically adjust the force in different cable routing phases.

In the future, we will introduce active perception with more side cameras to improve management of cable and gripper positions using dynamic parameters during robotic cable routing.

## ACKNOWLEDGMENT

We acknowledge the contribution of the motion library developed by Jacobi Robotics, and we appreciate the advice provided by Kavish Kondap, Jaimyn Drake and Pratyay Pandey.

## REFERENCES

- [1] T. Karlsson, E. Åblad, T. Hermansson, J. S. Carlson, and G. Tenfält, "Automatic cable harness layout routing in a customizable 3d environment," *Computer-Aided Design*, vol. 169, p. 103671, 2024.

- [2] J. Sanchez, J.-A. Corrales, B.-C. Bouzgarrou, and Y. Mezouar, "Robotic manipulation and sensing of deformable objects in domestic and industrial applications: a survey," *The International Journal of Robotics Research*, vol. 37, no. 7, pp. 688–716, 2018.
- [3] D. Seita, P. Florence, J. Tompson, E. Coumans, V. Sindhwani, K. Goldberg, and A. Zeng, "Learning to rearrange deformable cables, fabrics, and bags with goal-conditioned transporter networks," in *2021 IEEE International Conference on Robotics and Automation (ICRA)*. IEEE, 2021, pp. 4568–4575.
- [4] H. Mayer, F. Gomez, D. Wierstra, I. Nagy, A. Knoll, and J. Schmidhuber, "A system for robotic heart surgery that learns to tie knots using recurrent neural networks," *Advanced Robotics*, vol. 22, no. 13–14, pp. 1521–1537, 2008.
- [5] K. Shivakumar, V. Viswanath, A. Gu, Y. Avigal, J. Kerr, J. Ichnowski, R. Cheng, T. Kollar, and K. Goldberg, "Sgtm 2.0: Autonomously untangling long cables using interactive perception," in *2023 IEEE International Conference on Robotics and Automation (ICRA)*. London, UK: IEEE, May 29–June 2 2023.
- [6] S. Jin, W. Lian, C. Wang, M. Tomizuka, and S. Schaal, "Robotic cable routing with spatial representation," *IEEE Robotics and Automation Letters*, vol. 7, no. 2, pp. 5687–5694, 2022.
- [7] P. Mitrano and D. Berenson, "The grasp loop signature: A topological representation for manipulation planning with ropes and cables," in *2024 IEEE International Conference on Robotics and Automation (ICRA)*. IEEE, 2024, pp. 10 888–10 894.
- [8] Y. She, S. Wang, S. Dong, N. Sunil, A. Rodriguez, and E. Adelson, "Cable manipulation with a tactile-reactive gripper," *The International Journal of Robotics Research*, vol. 40, no. 12–14, pp. 1385–1401, 2021.
- [9] R. Hoque, K. Shivakumar, S. Aeron, G. Deza, A. Ganapathi, A. Wong, J. Lee, A. Zeng, V. Vanhoucke, and K. Goldberg, "Learning to fold real garments with one arm: A case study in cloud-based robotics research," in *2022 IEEE/RSJ International Conference on Intelligent Robots and Systems (IROS)*. IEEE, 2022, pp. 251–257.
- [10] C. Zhou, H. Xu, J. Hu, F. Luan, Z. Wang, Y. Dong, Y. Zhou, and B. He, "Ssfold: Learning to fold arbitrary crumpled cloth using graph dynamics from human demonstration," *IEEE Transactions on Automation Science and Engineering*, 2025.
- [11] L. Y. Chen, B. Shi, D. Seita, R. Cheng, T. Kollar, D. Held, and K. Goldberg, "Autobag: Learning to open plastic bags and insert objects," in *2023 International Conference on Robotics and Automation (ICRA)*. IEEE, 2023, pp. 3918–3925.
- [12] N. Gu, Z. Zhang, R. He, and L. Yu, "Shakingbot: dynamic manipulation for bagging," *Robotica*, vol. 42, no. 3, pp. 775–791, 2024.
- [13] P. Zhou, P. Zheng, J. Qi, C. Li, H.-Y. Lee, Y. Pan, C. Yang, D. Navarro-Alarcon, and J. Pan, "Bimanual deformable bag manipulation using a structure-of-interest based neural dynamics model," *IEEE/ASME transactions on mechatronics*, 2024.
- [14] K. Hari, H. Kim, W. Panitch, K. Srinivas, V. Schorp, K. Dharmarajan, S. Ganti, T. Sadjadpour, and K. Goldberg, "Stitch: Augmented dexterity for suture throws including thread coordination and handoffs," in *2024 International Symposium on Medical Robotics (ISMR)*. IEEE, 2024, pp. 1–7.
- [15] Z. Chen, K. Hari, T. Dasari, K. Shieh, R. Jain, D. M. Fer, G. Guthart, and K. Goldberg, "Surgical d-knot: Augmented dexterity for tying double knots by monitoring optical flow in monocular attention windows," in *2025 IEEE/RSJ International Conference on Intelligent Robots and Systems (IROS)*. IEEE, 2025.
- [16] H. Yin, A. Varava, and D. Kragic, "Modeling, learning, perception, and control methods for deformable object manipulation," *Science Robotics*, vol. 6, no. 54, 2021.
- [17] J. Mahler, M. Matl, V. Satish, M. Danielczuk, B. DeRose, S. McKinley, and K. Goldberg, "Learning ambidextrous robot grasping policies," *Science Robotics*, vol. 4, no. 26, 2019.
- [18] W. Yan, A. Vangipuram, P. Abbeel, and L. Pinto, "Learning predictive representations for deformable objects using contrastive estimation," in *Conference on Robot Learning*. PMLR, 2021, pp. 564–574.
- [19] K. Black, N. Brown, D. Driess, A. Esmail, M. Equi, C. Finn, N. Fusai, L. Groom, K. Hausman, B. Ichter *et al.*, " $\pi$ .0: A vision-language-action flow model for general robot control," in *Proceedings of Robotics: Science and Systems (RSS)*, 2025.
- [20] C. Cheang, S. Chen, Z. Cui, Y. Hu, L. Huang, T. Kong, H. Li, Y. Li, Y. Liu, X. Ma *et al.*, "Gr-3 technical report," *arXiv preprint arXiv:2507.15493*, 2025.
- [21] K. Black, N. Brown, J. Darpinian, K. Dhabalia, D. Driess, A. Esmail, M. Equi, C. Finn, N. Fusai, M. Y. Galliker *et al.*, " $\pi$ 0. 5: a vision-language-action model with open-world generalization," *arXiv preprint arXiv:2504.16054*, 2025.
- [22] M. Burgess and E. H. Adelson, "Grasp everything (get): 1-dof, 3-fingered gripper with tactile sensing for robust grasping," *arXiv preprint arXiv:2505.09771*, 2025.
- [23] S. Yuan, A. D. Epps, J. B. Nowak, and J. K. Salisbury, "Design of a roller-based dexterous hand for object grasping and within-hand manipulation," in *2020 IEEE International Conference on Robotics and Automation (ICRA)*. IEEE, 2020, pp. 8870–8876.
- [24] A. Bicchi, A. Marigo, and D. Prattichizzo, "Dexterity through rolling: Manipulation of unknown objects," in *Proceedings 1999 IEEE International Conference on Robotics and Automation (Cat. No. 99CH36288C)*, vol. 2. IEEE, 1999, pp. 1583–1588.
- [25] K. Y. Goldberg and M. L. Furst, "Low friction gripper," Mar. 24 1992, US Patent 5,098,145.
- [26] B. Carlisle, K. Goldberg, A. Rao, and J. Wiegley, "A pivoting gripper for feeding industrial parts," in *Proceedings of the 1994 IEEE International Conference on Robotics and Automation*, 1994, pp. 1650–1655 vol.2.
- [27] V. Viswanath, K. Shivakumar, J. Kerr, B. Thananjeyan, E. Novoseller, J. Ichnowski, A. Escontrela, M. Laskey, J. E. Gonzalez, and K. Goldberg, "Autonomously untangling long cables," in *Proceedings of Robotics: Science and Systems (RSS)*, 2022. [Online]. Available: <https://roboticsconference.org/2022/program/papers/034/>
- [28] J. Luo, C. Xu, X. Geng, G. Feng, K. Fang, L. Tan, S. Schaal, and S. Levine, "Multistage cable routing through hierarchical imitation learning," *IEEE Transactions on Robotics*, vol. 40, pp. 1476–1491, 2024.
- [29] J. Zuo, B. Zhang, and F. Zhang, "Carobio: 3d cable routing with a bio-inspired gripper fingernail," in *2025 10th International Conference on Automation, Control and Robotics Engineering (CACRE)*. IEEE, 2025, pp. 72–79.
- [30] A. Wilson, H. Jiang, W. Lian, and W. Yuan, "Cable routing and assembly using tactile-driven motion primitives," in *Proceedings of the 2023 IEEE International Conference on Robotics and Automation (ICRA)*. London, UK: IEEE, May 29–June 2 2023, pp. 10 408–10 414.
- [31] M. Saha and P. Isto, "Manipulation planning for deformable linear objects," *IEEE Transactions on Robotics*, vol. 23, no. 6, pp. 1141–1150, 2007.
- [32] G. A. Walterson, R. Laezza, and Y. Karayiannidis, "Planning and control for cable-routing with dual-arm robot," in *2022 International Conference on Robotics and Automation (ICRA)*, 2022, pp. 1046–1052.
- [33] F. Süberkrüb, R. Laezza, and Y. Karayiannidis, "Feel the tension: Manipulation of deformable linear objects in environments with fixtures using force information," in *2022 IEEE/RSJ International Conference on Intelligent Robots and Systems (IROS)*. IEEE, 2022, pp. 11 216–11 222.
- [34] O. Azulay, K. Kondap, J. Drake, S. Xie, H. Li, S. Chitta, and K. Goldberg, "Motorcycle 1.0: Automating bimanual cable routing around fixtures on the nist task board," in *2025 IEEE 21st International Conference on Automation Science and Engineering (CASE)*, 2025.
- [35] K. Kimble, K. Van Wyk, J. Falco, E. Messina, Y. Sun, M. Shibata, W. Uemura, and Y. Yokokohji, "Benchmarking protocols for evaluating small parts robotic assembly systems," *IEEE robotics and automation letters*, vol. 5, no. 2, pp. 883–889, 2020.
- [36] V. Viswanath, K. Shivakumar, M. Parulekar, J. Ajmera, J. Kerr, J. Ichnowski, R. Cheng, T. Kollar, and K. Goldberg, "Handloom: Learned tracing of one-dimensional objects for inspection and manipulation," in *Conference on Robot Learning*. PMLR, 2023, pp. 341–357.
- [37] A. Bundy and L. Wallen, "Breadth-first search," in *Catalogue of artificial intelligence tools*. Springer, 1984, pp. 13–13.
- [38] M. A. Fischler and R. C. Bolles, "Random sample consensus: a paradigm for model fitting with applications to image analysis and automated cartography," *Communications of the ACM*, vol. 24, no. 6, pp. 381–395, 1981.